第 34 卷第 3 期 无 机 化 学 学 报 Vol.34 No.3
2018 年 3 月 CHINESE JOURNAL OF INORGANIC CHEMISTRY 515-524

三维超分子锌/锰配合物的合成、晶体结构及理论计算

王志涛[1,2] 瓦伦丁·瓦尔切夫*[,2] 方千荣[2] 李秀梅[1] 潘亚茹[1]
([1]通化师范学院化学学院,通化 134002)
([2]吉林大学无机合成与制备化学国家重点实验室,长春 130012)

摘要:通过水热法合成了 2 个新的三维超分子配合物{[Zn_2(pzdc)(L)$_2$(H_2O)]·H_2O}$_n$ (**1**)和[Mn(μ_2-O)(H_2O)$_2$(HL)]·NIPH (**2**)(H_2pzdc=吡嗪-2,3-二甲酸,H_2NIPH=5-硝基间苯二甲酸,HL=3-(2-吡啶基)吡唑))。并对其进行了元素分析、红外光谱、紫外光谱、热重、荧光光谱、X 射线单晶和粉末衍射测定。配合物 **1** 是二维网状结构,配合物 **2** 为零维结构,这 2 个配合物通过氢键和 π-π 相互作用形成了三维超分子网状结构。此外,还用高斯 09 程序 PBE0/LANL2DZ 方法对配合物 **1** 和 **2** 进行了自然键轨道(NBO)分析,计算结果表明配位原子与 Zn、Mn 离子之间存在着共价作用。

关键词:水热合成;晶体结构;锌配合物;锰配合物;自然键轨道
中图分类号:O614.24+1;O614.71+1 **文献标识码**:A **文章编号**:1001-4861(2018)03-0515-10
DOI:10.11862/CJIC.2018.038

Syntheses, Crystal Structures and Theoretical Calculation of Three-Dimensional Supramolecular Zinc/Manganese Complex

WANG Zhi-Tao[1,2] Valentin Valtchev*[,2] FANG Qian-Rong[2] LI Xiu-Mei[1] PAN Ya-Ru[1]
([1]*Faculty of Chemistry, Tonghua Normal University, Tonghua, Jilin* 134002, *China*)
([2]*State Key Laboratory of Inorganic Synthesis and Preparative Chemistry, Jilin University, Changchun* 130012, *China*)

Abstract: Two new three-dimensional supramolecular complexes {[Zn_2(pzdc)(L)$_2$(H_2O)]·H_2O}$_n$ (**1**) and [Mn(μ_2-O)(H_2O)$_2$(HL)]·NIPH (**2**) (H_2pzdc=pyrazine-2,3-dicarboxylic acid, H_2NIPH=5-nitroisophthalic acid, HL=3-(2-pyridyl) pyrazole) have been hydrothermally synthesized and structurally characterized by elemental analysis, IR spectrum, UV spectrum, TG, fluorescence spectrum, single-crystal and powder X-ray diffraction. Complex **1** shows two-dimensional (2D) network, and complex **2** is zero-dimensional structure. They are further extended into a three-dimensional supramolecular network structure through hydrogen bonds and π-π interactions. Moreover, natural bond orbital (NBO) was analyzed by using the PBE0/LANL2DZ method built in Gaussian 09 program. The calculation results indicate the distinct covalent interaction between the coordinated atoms and Zn(Ⅱ), Mn(Ⅱ) ion, respectively. CCDC: 1468826, **1**; 1439401, **2**.

Keywords: hydrothermal synthesis; crystal structure; Zn(Ⅱ) complex; Mn(Ⅱ) complex; natural bond orbital

The design and synthesis of metal-organic coordination polymers relying on the selection of ligands and metal ions have become a very attractive research field. This is motivated not only by the intriguing structural diversity but also by the demand of applying functional materials into the fields of catalysis, porosity, magnetism, luminescence and nonlinear optics[1-3]. In general, grids with various sizes and shapes

收稿日期:2017-08-07。收修改稿日期:2017-11-13。
吉林省教育厅科学技术研究(吉教科合字[2013]第 384 号)和吉林省科技发展计划(No.201205080)资助项目。
*通信联系人。E-mail:laowa2017@163.com

can be synthesized by choosing suitable single metal ions and organic ligands such as carboxylates and N-donor groups[4-6]. Self-assembly is a complex process, highly influenced by many factors, such as the coordination geometry of metal ions, the nature of organic ligands, solvent system, temperature, pH value of the solution, the ratio between metal salt and ligand, the templates and the counter anions[7-14]. Except for these factors, other forces such as hydrogen-bonding, π-π interactions, metal-metal interactions can also greatly influence the supramolecular topology and its dimensionality[15-17]. Therefore, these considerations made us investigate new coordination structures with pyrazine-2,3-dicarboxylic acid, 5-nitroisophthalic acid and chelating ligands. In this manuscript, we reported the syntheses, crystal structures, IR, UV, fluorescence, TG properties of two new complexes, namely, $\{[Zn_2(pzdc)(L)_2(H_2O)]\cdot H_2O\}_n$ (**1**) and $[Mn(\mu_2\text{-}O)(H_2O)_2(HL)]\cdot NIPH$ (**2**). Moreover, we analyzed natural bond orbital (NBO) by using the PBE0/LANL2DZ method built in Gaussian 09 program.

1 Experimental

1.1 General procedures

All solvents and chemicals were commercial reagents and used without further purification. Elemental analyses (carbon, hydrogen, and nitrogen) were performed with a Vario EL Ⅲ Elemental Analyzer. IR spectrum (4 000~400 cm^{-1}) was measured from KBr pellet on a Nicolet 6700 FT-IR spectrometer. TG studies were performed on a Perkin-Elmer TGA7 analyzer. UV spectrum was obtained on a Shimzu UV-250 spectrometer in the 200~400 nm range. The fluorescent studies were carried out on a computer-controlled JY Fluoro-Max-3 spectrometer at room temperature. The crystal structure was determined by a Bruker D8 Venture diffractometer. The powder X-ray diffraction (PXRD) studies were performed with a Bruker D8 Discover instrument (Cu $K\alpha$ radiation, λ= 0.154 184 nm, U=40 kV, I=40 mA) over the 2θ range of 5°~50° at room temperature.

1.2 Synthesis

$\{[Zn_2(pzdc)(L)_2(H_2O)]\cdot H_2O\}_n$ (**1**): A mixture of H_2pzdc (0.068 g, 0.4 mmol), HL (0.028 g, 0.2 mmol), $Zn(OAc)_2\cdot 2H_2O$ (0.088 g, 0.4 mmol) and 18 mL H_2O was adjust to the pH≈6.13 with 0.5 $mol\cdot L^{-1}$ NaOH, sealed in a Teflon-lined stainless steel vessel, heated to 160 ℃ for five days, and followed by slow cooling (a descent rate of 10 $℃\cdot h^{-1}$) to room temperature. Pale yellow block crystals were obtained. Yield: 32% (based on Zn). Anal. Calcd. for $C_{44}H_{32}N_{16}O_{11}Zn_4$(%): C, 43.23; H, 2.64; N, 18.33. Found (%): C, 42.97; H, 2.15; N, 17.89. IR (cm^{-1}): 3 286(w), 2 989(w), 1 752 (m), 1 637(m), 1 605(m), 1 567(w), 1 473(w), 1 434 (w), 1 375(m), 1 357(m), 1 255(w), 1 159(w), 1 118 (w), 1 060(w), 1 013(m), 890(w), 783(w), 765(w), 636 (w), 481(w).

$[Mn(\mu_2\text{-}O)(H_2O)_2(HL)]\cdot NIPH$ (**2**): A mixture of $Mn(OAc)_2\cdot 4H_2O$ (0.10 g, 0.4 mmol), H_2NIPH (0.084 g, 0.4 mmol), HL (0.058 g, 0.4 mmol) and 18 mL H_2O was placed in a Teflon reactor (30 mL) and the pH value was adjusted to about 7 with 0.5 $mol\cdot L^{-1}$ NaOH solution. Then the mixture was heated at 140 ℃ for 7 days. After cooling to room temperature at a rate of 10 $℃\cdot h^{-1}$, brown crystals of **1** were collected in 45% yield. Anal. Calcd. for $C_{32}H_{30}Mn_2N_8O_{18}$(%):C, 41.57; H, 3.27; N, 12.12. Found(%): 41.36; H, 3.01; N, 11.98. IR (KBr, cm^{-1}): 3 413(m), 3 102(w), 1 630(s), 1 606(s), 1 583(m), 1 533(m), 1 495(w), 1 443(w), 1 334(s), 1 101(w), 998(w), 788(w), 720(m), 537(w).

1.3 X-ray crystallography

Single-crystal X-ray diffraction data for **1** and **2** were measured on a Bruker Smart Apex Ⅱ CCD diffractometer with graphite-monochromated Mo Kα radiation (λ=0.071 073 nm) at 293 K. The structure was solved with the direct method of SHELXS-97 and refined with full-matrix least-squares techniques using the SHELXL-97 program[18-19]. Anisotropic thermal parameters were assigned to all non-hydrogen atoms. The hydrogen atoms were placed at the calculated positions and refined as riding atoms with isotropic displacement parameters. The details of the crystal parameters, data collection and refinement for **1** and **2** are summarized in Table 1. Selected bond lengths and bond angles are shown in Table 2.

CCDC: 1468826, 1; 1439401, 2.

Table 1　Crystal data and structure refinement for 1 and 2

Complex	1	2
Formula	$C_{44}H_{32}N_{16}O_{11}Zn_4$	$C_{32}H_{30}Mn_2N_8O_{18}$
Formula weight	1 223.34	924.52
Crystal system	Monoclinic	Triclinic
Space group	*C*2/*c*	$P\bar{1}$
a / nm	2.946 5(2)	0.751 93(5)
b / nm	1.241 03(8)	1.078 08(6)
c / nm	1.470 59(9)	1.149 68(7)
α / (°)		88.388 0(10)
β / (°)	117.727(2)	86.926 0(10)
γ / (°)		85.592 0(10)
Volume / nm^3	4.760 1(6)	0.927 61(10)
Z	4	1
D_c / (g·cm^3)	1.707	1.655
θ range / (°)	3.12~25.09	1.77~26.06
F(000)	2 468	472
Reflections collected, unique	15 191, 4 206	5 118, 3 611
Goodness-of-fit on F^2	1.012	1.110
R_{int}	0.049 1	0.010 0
R_1, wR_2 [$I>2\sigma(I)$]	0.0334 8, 0.071 3	0.029 1, 0.077 9

Table 2　Selected bond lengths (nm) and bond angles (°) for 1 and 2

		1			
Zn(1)-O(1)	0.207 9(2)	Zn(1)-O(4A)	0.212 5(2)	Zn(1)-O(5)	0.198 9(2)
Zn(1)-N(2A)	0.210 3(2)	Zn(1)-N(8)	0.200 7(3)	Zn(2)-N(3)	0.218 0(3)
Zn(2)-N(4)	0.208 5(3)	Zn(2)-N(5B)	0.206 3(3)	Zn(2)-N(6)	0.222 2(3)
Zn(2)-N(7)	0.210 2(3)				
O(5)-Zn(1)-N(8)	115.11(12)	O(5)-Zn(1)-O(1)	91.16(9)	N(5)-Zn(1)-O(1)	93.51(10)
O(5)-Zn(1)-N(2A)	137.52(12)	N(8)-Zn(1)-N(2A)	104.72(11)	O(1)-Zn(1)-N(2A)	100.89(9)
O(5)-Zn(1)-O(4A)	84.53(9)	N(8)-Zn(1)-O(4A)	95.61(10)	O(1)-Zn(1)-O(4A)	170.86(10)
N(2A)-Zn(1)-O(4A)	77.26(9)	N(5B)-Zn(2)-N(4)	97.81(10)	N(5B)-Zn(2)-N(7)	92.80(10)
N(4)-Zn(2)-N(7)	169.10(10)	N(5B)-Zn(2)-N(3)	170.89(11)	N(4)-Zn(2)-N(3)	76.88(10)
N(7)-Zn(2)-N(3)	92.92(10)	N(5B)-Zn(2)-N(6)	100.58(11)	N(4)-Zn(2)-N(6)	99.62(11)
N(7)-Zn(2)-N(6)	75.85(11)	N(3)-Zn(2)-N(6)	87.69(11)		
		2			
Mn(1)-O(7)	0.213 46(14)	Mn(1)-O(8)	0.223 76(13)	Mn(1)-O(8A)	0.233 36(14)
Mn(1)-O(9)	0.214 69(13)	Mn(1)-N(2)	0.222 64(14)	Mn(1)-N(3)	0.225 56(14)
O(7)-Mn(1)-O(9)	89.28(6)	O(7)-Mn(1)-O(2)	93.03(5)	O(9)-Mn(1)-N(2)	170.50(6)
O(7)-Mn(1)-O(8)	93.40(5)	O(9)-Mn(1)-O(8)	93.97(5)	O(2)-Mn(1)-O(8)	95.09(5)
O(7)-Mn(1)-N(3)	101.62(6)	O(9)-Mn(1)-N(3)	96.56(5)	N(2)-Mn(1)-N(3)	73.95(5)
O(8)-Mn(1)-N(3)	161.72(5)	O(7)-Mn(1)-O(8A)	168.77(5)	O(9)-Mn(1)-O(8A)	85.12(5)
N(2)-Mn(1)-O(8A)	94.09(5)	O(8)-Mn(1)-O(8A)	77.32(5)	N(3)-Mn(1)-O(8A)	88.71(5)

Symmetry codes: A: *x*, 1−*y*, *z*−1/2; B: −*x*+3/2, −*y*+1/2, 1−*z* for **1**; A: −1−*x*, 2−*y*, −*z* for **2**.

2 Results and discussion

2.1 IR spectrum

For complex **1**, two bands at 1 637 and 1 357 cm^{-1} can be attributed to $\nu(OCO)_{assym}$ and $\nu(OCO)_{sym}$[20], respectively. The $\Delta\nu$ ($\nu(OCO)_{assym}$–$\nu(OCO)_{sym}$) is 280 cm^{-1}, exhibiting the presence of monodentate ($\Delta\nu$>200 cm^{-1}) linkage of carboxylates in the dianions. Therefore, the carboxylates coordinate to the metal as monodentate ligands via the carboxylate groups[21]. The absence of the characteristic bands at abound 1 700 cm^{-1} in complex **1** owing to the protonated carboxylic group indicates the complete deprotonation of pzdc ligand upon reaction with Zn ions[22]. Moreover, X-ray diffraction analysis further attributes the existence of monodentate coordination manners of the carboxylate groups and prence deprotonation of pzdc ligands.

Infrared spectroscopy of complex **2** shows the typical anti-symmetric (1 606 cm^{-1}) and symmetric (1 334 cm^{-1}) stretching bands of carboxylate groups. The absence of the characteristic band around 1 700 cm^{-1} in complex **2** owing to the protonated carboxylic group indicates that the present deprotonation of NIPH ligand. Moreover, the strong and broad band centered at 3 413 cm^{-1} for **2** is owing to the H-O-H stretching vibration of water molecule in the light of the known structure[23].

2.2 Description of the structure

X-ray single-crystal diffraction analysis reveals that **1** crystallizes in the monoclinic system, space group *C*2/*c* and features a 2D network structure. The coordination environment of Zn(Ⅱ) in **1** is displayed in Fig.1. There are two coordination centers, Zn1 and Zn2, in the crystal structure. The Zn1 ion is five-coordinated by two carboxylate oxygen atoms (O1, O4A) from two different pzdc ligands, two nitrogen donors (N2A, N8) from pzdc and HL ligands and one coordinated water molecule (O5). The Zn2 ion is also five-coordinated by five nitrogen atoms (N3, N4, N5B, N6, N7). The Zn-O distances fall in the range of 0.198 9(2)~0.212 5(2) nm, and Zn-N bond length fall in the 0.200 7(3)~0.222 2(3) nm, which are all in the normal ranges and the coordination angles around Zn atom are in the range 75.86(11)°~170.90(11)°.

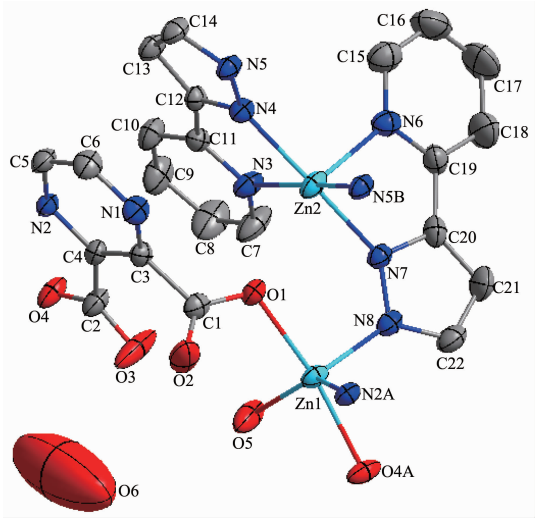

Thermal ellipsoids at 50% probability; Symmetry codes: A: *x*, 1−*y*, *z*−1/2; B: −*x*+3/2, −*y*+1/2, 1−*z*

Fig.1 ORTEP drawing of **1** showing the local coordination environment of Zn(Ⅱ)

In the crystal structure of complex **1**, the HL ligands take μ_3 coordination mode and the completely deprotonated pzdc ligands show one kind of coordination mode, namely, monodentate bridging mode. As a result, two Zn(Ⅱ) ions are linked by four HL ligand to form dinuclear subunits, which are bridged by pzdc ligands to yield a two-dimensional (2D) network architecture (Fig.2). Each Zn(Ⅱ) shows a

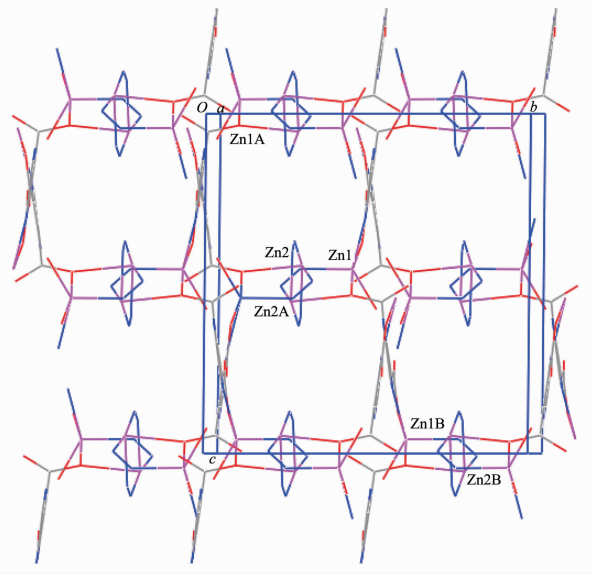

Carbon atoms and one nitrogen atom of HL ligand were omitted for clarity; Symmetry codes: A: *x*, 1−*y*, *z*−1/2; B: −*x*+3/2, −*y*+1/2, 1−*z*

Fig.2 View of the two-dimensional network along *a* axis

distorted square-pyramidal coordination structure.

It is worth noting that hydrogen bonding interactions are important in the synthesis of supramolecular architecture [24]. There are O–H⋯O and C–H⋯O hydrogen bonding interactions between carboxylate oxygen atom, carbon atoms and coordinated water molecules in complex **1** (Table 3). In addition, there are π-π interactions (Fig.3) in complex **1** between pyrazine ring of pzdc ligand and pyrazole ring of HL ligand. The centroid-to-centroid distance between adjacent ring is 0.345 6(2) nm for N4N5C14C13C12 and N1C3C4N2C5C6 rings. The perpendicular distance is 0.315 30(15) nm for N4N5C14C13C12 and N1C3C4N2C5C6 rings. Thus, the two-dimensional networks are further extended into a three-dimensional supramolecular framework through hydrogen bonds and π-π interactions, which play an important role in stabilizing compound **1**.

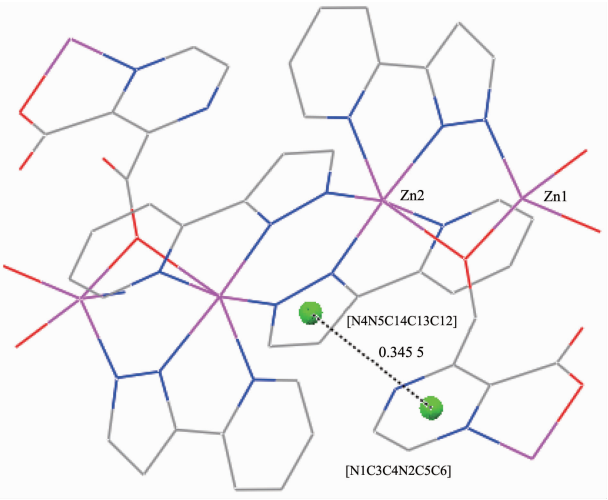

Fig.3　View of π-π stacking interactions in complex **1**

Complex **2** crystallizes in the triclinic system, space group $P\bar{1}$ and features a zero-dimensional structure. The coordination environment of Mn(Ⅱ) in 2 is displayed in Fig.4. There are two Mn(Ⅱ) ion, two NIPH ligand, two HL ligand, four coordinated water molecule and two μ_2-O atoms in the molecular structure. Each Mn(Ⅱ) ion is six-coordinated by two coordinated water molecules (O7, O9), two μ_2-O atoms (O8, O8A) and two nitrogen donors (N2 and N3) from HL ligand to supply a distorted octahedral coordination structure. One coordinated water molecule (O9), one μ_2-O atom (O8) and two nitrogen atoms (N2, N3) define an equatorial plane, whereas the axial coordination sites are employed by the other coordinated water molecule (O7) and μ_2-O atom (O8A). The Mn-O distances fall in the range of 0.213 46(14)~0.233 36(14) nm, and Mn-N bond length fall in the 0.222 64(14)~0.225 56(14) nm, which are all in the normal range and the

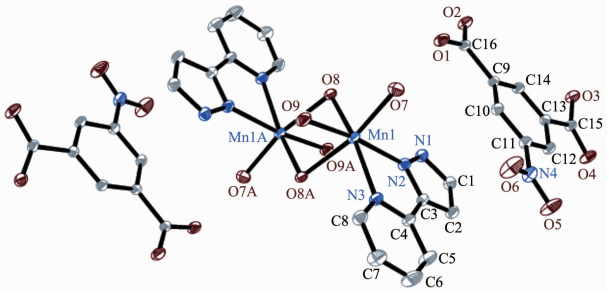

Thermal ellipsoids at 30% probability; Symmetry codes: A: $-x-1$, $-y+2$, $-z$

Fig.4　ORTEP drawing of **2** showing the local coordination environment of Mn(Ⅱ)

Table 3　Hydrogen bond parameters for complexes 1 and 2

D–H⋯A	*d*(D-H) / nm	*d*(H⋯A) / nm	*d*(D⋯A) / nm	∠DHA / (°)
		1		
O(5)–H(W1)⋯O(3)	0.085	0.229	0.262 0(4)	103
O(5)–H(W2)⋯O(4)	0.085	0.209	0.282 3(4)	145
C(10)–H(10)⋯O(2)	0.085(4)	0.242(4)	0.324 8(5)	164(3)
C(17)–H(17)⋯O(2)	0.091(5)	0.258(5)	0.331 7(6)	139(4)
		2		
N(1)–H(3)⋯O(3)	0.098(2)	0.178(2)	0.273 8(2)	166.6(19)
O(7)–H(W1)⋯O(1)	0.084(3)	0.186(3)	0.269 20(19)	174(3)
O(7)–H(W21)⋯O(4)	0.078(3)	0.191(3)	0.267 71(19)	173(2)
O(9)–H(W3)⋯O(3)	0.064(2)	0.196(2)	0.259 62(18)	173(2)
O(9)–H(W4)⋯O(2)	0.087(3)	0.178(3)	0.264 18(19)	169(3)

coordination angles around Mn(Ⅱ) ion are in the range of 73.95(5)°~168.77(5)°.

In **2**, the HL ligand adopts classic chelating mode, while NIPH ligand was not involved in coordination, which just play a role of balance charge. Two Mn(Ⅱ) ions are linked by two μ_2-O atoms to form dinuclear subunits, and exhibits zero-dimensional structure. Further study of the crystal packing of complex **2** suggests that there are two kinds of N–H⋯O and O–H ⋯ O hydrogen bonding interactions between nitrogen atom of HL ligand, carboxylate oxygen atoms of NIPH ligand, and coordinated water molecule (Table 3). Moreover, In complex **2**, 5-member ring of HL and 6-member ring of NIPH ligand centroid distances are 0.368 79(10) nm for N1N2C3C2C1 and C9C10C11C12C13C14 rings, with the vertical distance of 0.326 64(7) nm, indicating the existence of π-π effect, so the structure is more stable. Therefore, a three-dimensional supramolecular network structure is formed by such hydrogen bonds and π-π stacking (Fig.5).

In order to check the purity of complex **1** and **2**, powder X-ray diffraction of the as-synthesized sample were measured at room temperature (Fig.6). The peak positions of experimental patterns are in good agreement with the simulated ones, which clearly indicates good purity of **1** and **2**[25-26].

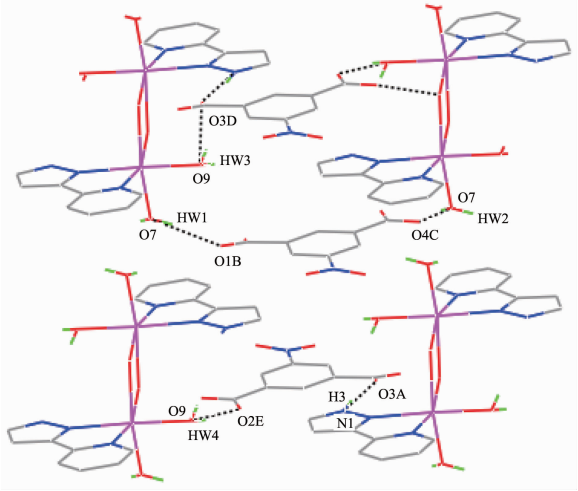

Symmetry codes: A: x, y, $1+z$; B: $-x$, $1-y$, $1-z$; C: $-x$, $-y$, $1-z$; D: $1-x$, $-y$, $1-z$; E: x, $-1+y$, $1+z$

Fig.5 View of the 3D supramolecular architecture of **2** formed by hydrogen-bonding and π-π interactions

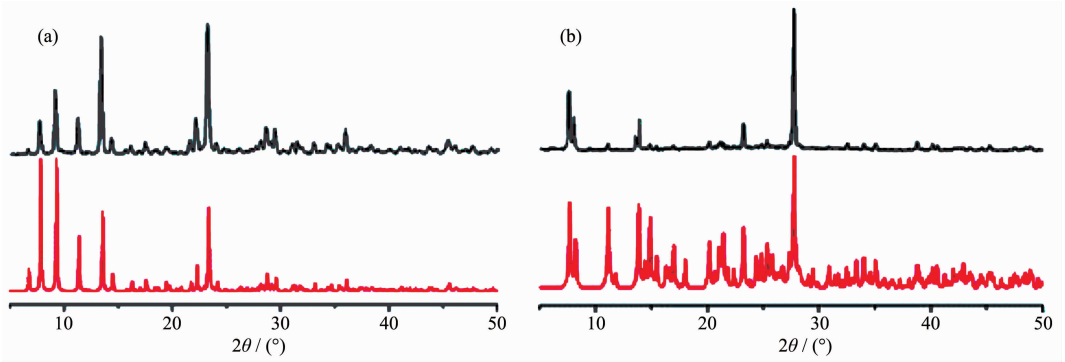

Bottom: simulated; Top: experimental

Fig.6 PXRD analysis of complex **1** (a) and **2** (b)

2.3 Thermal analysis

The thermal stability of complex **1** was tested in the range of 50~700 ℃ under a nitrogen atmosphere at a heating rate of 5 ℃·min^{-1}. The TGA curve of complex **1** is shown in Fig.7. It displays that the first weight loss of 49.5% from 60 to 192 ℃ corresponds to the release of water molecules and HL ligand (Calcd. 50.0%). Upon further heating, an obvious weight loss (26.2%) occurs in the temperature range of 192~525 ℃, corresponding to the removal of pzdc ligands (Calcd. 27.1%). After 525 ℃ no weight loss is found, which indicates the complete decomposition of **1**.

2.4 Photoluminescent properties

The emission spectrum of complex **1** in the solid state at room temperature is displayed in Fig.8. It can be reviewed that complex **1** shows blue photoluminescence with an emission maximum at *ca.* 460 nm upon excitation at 375 nm. By way of studying the

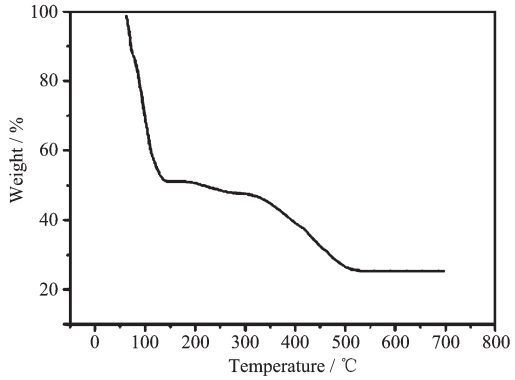

Fig.7　TG curve of the complex **1**

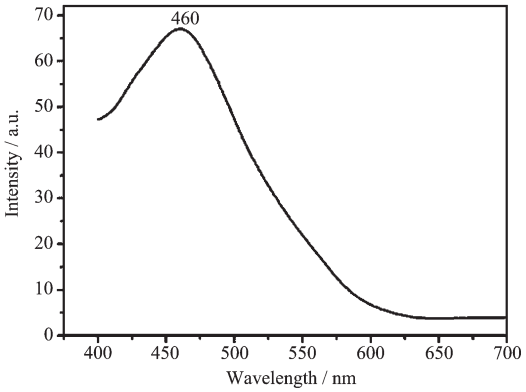

Fig.8　Solid-state emission spectrum of **1** at room temperature

nature of these emission bands, we first investigated the photoluminescence properties of free H_2pzdc, and the result indicated that it does not emit any luminescence in the range of 400~800 nm. And then we discussed the emission spectrum of HL itself and the result confirmed that it does not emit any luminescence in the range 400~800 nm, which has also been proved previously[27]. Therefore, on the basis of previous literature[28], the emission band could be assigned to the emission of ligand-to-metal charge transfer (LMCT). For possessing strong fluorescent intensity, complex **1** appears to be good candidates for novel hybrid inorganic-organic photoactive materials.

2.5　UV spectrum analysis

The UV spectra for complex **2** (Fig.9), H_2NIPH and HL ligands have been studied in the solid state. For H_2NIPH and HL ligands, there are 277 and 245 nm absorption bands, respectively, while 275 nm for complex **2**, which should be assigned to the $n\rightarrow\pi^*$[29-32] transition of HL ligand in **2**. However, after the ligands coordinates to the Mn^{2+} ion, the absorption intensity increases.

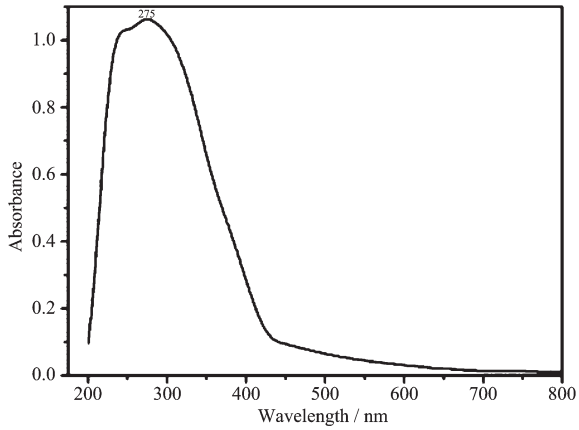

Fig.9　UV spectrum of **2** at room temperature

2.6　Theoretical calculations

All calculations in this work were carried out with the Gaussian 09 program[33]. The parameters of the molecular structure for calculation were all from the experimental data of the complex. We analyzed natural bond orbital (NBO) by density functional theory (DFT)[34] with the PBE0[35-38] hybrid functional and the LANL2DZ basis set[39].

The selected natural atomic charges and natural electron configuration for the complex **1** are displayed in Table 4. It is showed that the electronic configurations of Zn(Ⅱ) ion, N and O atoms are $4s^{0.30}3d^{9.98}4p^{0.40}$, $2s^{1.32\sim1.37}2p^{4.06\sim4.23}$ and $2s^{1.64\sim1.69}2p^{5.11\sim5.23}$, respectively. On the basis of above results, one can conclude that the Zn(Ⅱ) ion coordinated with N and O atoms is mostly on 3*d*, 4*s*, and 4*p* orbitals. N atoms form coordination bonds with Zn(Ⅱ) ion using 2*s* and 2*p* orbitals. All O atoms provide electrons of 2*s* and 2*p* to Zn(Ⅱ) ion and form the coordination bonds. Thus, the Zn(Ⅱ) ion obtained some electrons from N atoms and O atoms of ligands[40-41]. Therefore, on the basis of valence-bond theory, the atomic net charges distribution of the complex **1** appears the obvious covalent interaction between the coordinated atoms and Zn(Ⅱ) ion.

As can be seen from the Fig.10, lowest unoccupied molecular orbital (LUMO) is mainly consists of HL and H_2pzdc ligands, whereas highest occupied molecular orbital (HOMO) mostly composed of HL ligand. So, the charge transfer from ligand to

ligand may be deduced from some contours of molecular orbital of complex **1**.

Table 4 Selected natural atomic charges and natural electron configuration for 1 and 2

Atom	Net charge	Electron configuration
	1	
Zn(1)	1.318 25	[core]$4s^{0.30}3d^{9.98}4p^{0.40}$
O(1)	−0.797 20	[core]$2s^{1.67}2p^{5.12}$
O(4A)	−0.810 76	[core]$2s^{1.69}2p^{5.11}$
O(5)	−0.882 56	[core]$2s^{1.64}2p^{5.23}$
N(2A)	−0.528 29	[core]$2s^{1.33}2p^{4.18}$
N(8)	−0.449 17	[core]$2s^{1.37}2p^{4.06}$
Zn(2)	1.320 12	[core]$4s^{0.30}3d^{9.98}4p^{0.40}$
O(1)	−0.797 20	[core]$2s^{1.67}2p^{5.12}$
N(3)	−0.567 85	[core]$2s^{1.32}2p^{4.23}$
N(4)	−0.458 82	[core]$2s^{1.35}2p^{4.08}$
N(5B)	−0.494 30	[core]$2s^{1.36}2p^{4.11}$
N(6)	−0.527 33	[core]$2s^{1.33}2p^{4.18}$
N(7)	−0.432 72	[core]$2s^{1.35}2p^{4.06}$
	2	
Mn(1)	0.465 62	[core]$4s^{0.23}3d^{5.82}5p^{0.43}$
O(7)	−0.801 50	[core]$2s^{1.63}2p^{5.15}$
O(8)	−0.798 61	[core]$2s^{1.87}2p^{4.92}$
O(8A)	−0.777 44	[core]$2s^{1.87}2p^{4.90}$
O(9)	−0.802 55	[core]$2s^{1.61}2p^{5.18}$
N(2)	−0.251 63	[core]$2s^{1.35}2p^{3.88}$
N(3)	−0.441 78	[core]$2s^{1.32}2p^{4.10}$

Symmetry codes: A: x, $1-y$, $z-1/2$; B: $-x+3/2$, $-y+1/2$, $1-z$ for **1**; A: $-x-1$, $-y+2$, $-z$ for **2**.

The selected natural atomic charges and natural electron configuration for complex **2** is displayed in Table 4. It is showed that the electronic configurations of Mn(Ⅱ) ion, N and O atoms are $4s^{0.23}3d^{5.82}5p^{0.43}$, $2s^{1.32\sim1.35}2p^{3.88\sim4.10}$ and $2s^{1.61\sim1.87}2p^{4.90\sim5.18}$, respectively. On the basis of above results, one can infer that the Mn(Ⅱ) ion coordination with N and O atoms is mostly on 3*d*, 4*s*, and 5*p* orbitals. N atoms form coordination bonds with Mn(Ⅱ) ion using 2*s* and 2*p* orbitals. All O atoms provide electrons of 2*s* and 2*p* to Mn(Ⅱ) ion and form the coordination bonds. Thus, the Mn(Ⅱ) ion obtained some electrons from two N atoms of HL ligand, two O atoms of coordinated water molecules, two μ_2-O atoms[40-41]. Therefore, on the basis of valence-bond theory, the atomic net charge distribution and the NBO bond orders of complex **2** (Table 4) exhibits the obvious covalent interaction between the coordinated atoms and Mn(Ⅱ) ion. The differences of the NBO bond orders for Mn-O and Mn-N bonds make their bond lengths be different[41], which is in good agreement with the X-ray crystal structural data of complex **2**.

As can be seen from the Fig.11, lowest unoccupied molecular orbital (LUMO) is mostly consists of HL ligand and metal, whereas highest occupied molecular orbital (HOMO) mainly composed of μ_2-O and metal center. So, the charge transfer from ligand to ligand and metal to ligand may be inferred from some contours of molecular orbital of complex **2**.

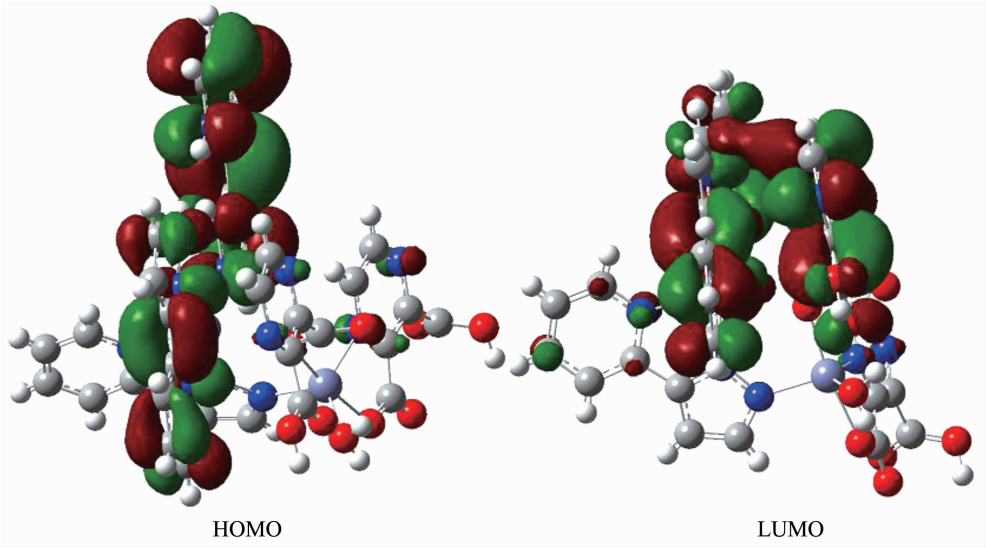

Fig.10 Frontier molecular orbitals of the complex **1**

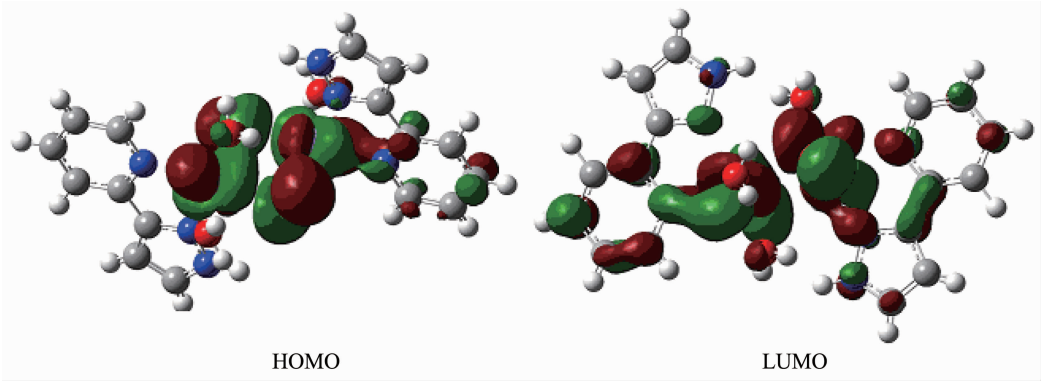

Fig.11 Frontier molecular orbitals of the complex **2**

3 Conclusions

In general, we have described two new supramolecular zinc/manganese complexes. In **1**, the pyrazine-2,3-dicarboxylate ligands function in monodentate bridging coordination mode, and the HL ligands take μ_3 coordination mode. As a result, two Zn(Ⅱ) ions are linked by four HL ligand to yield dinuclear subunits, which are bridged by pzdc ligands to form a two-dimensional network structure. In **2**, the HL ligand takes classic chelating mode, while NIPH ligand was not involved in coordination, which just plays a role of balance charge. Two Mn(Ⅱ) ions are linked by two μ_2-O atoms to form dinuclear subunits, and exhibits zero-dimensional structure. It is worthy to note that the intermolecular hydrogen bonds and π-π interactions play an important role in the supramolecular structure. These materials will give new impetus to the construction of novel functional material with potentially useful physical properties.

References:

[1] Uppadine L H, Lehn J M. *Angew Chem. Int. Ed.*, **2004**,**43**: 240-243

[2] WANG Qing-Wei(王庆伟), WANG Ya-Nan(王亚楠), LI Xiu-Mei(李秀梅), et al. *Chinese J. Inorg. Chem.*(无机化学学报), **2014**,**30**(9):2219-2224

[3] Hou L, Li D, Shi W J, et al. *Inorg. Chem.*, **2005**,**44**:7825-7832

[4] Hines C C, Reichert W M, Griffin S T. *J. Mol. Struct.*, **2006**, **796**:76-85

[5] Wang X L, Qin C,Wang E B, et al. *Chem. Eur. J.*, **2006**,**12**: 2680-2691

[6] García-Couceiro U, Castillo O, Luque A, et al. *Cryst. Growth Des.*, **2006**,**6**:1839-1847

[7] Hong M C, Zhao Y J, Su W P, et al. *Angew. Chem. Int. Ed.*, **2000**,**39**:2468-2470

[8] Hong M C, Zhao Y Z, Su W P, et al. *J. Am. Chem. Soc.*, **2000**,**122**:4819-4820

[9] Abrahams B F, Batten S R, Grannas M J, et al. *Angew. Chem. Int. Ed.*, **1999**,**38**:1475-1477

[10]Bu X H, Chen W, Lu S L, et al. *Angew. Chem. Int. Ed.*, **2001**,**40**:3201-3203

[11]Noro S, Kitaura R, Kondo M, et al. *J. Am. Chem. Soc.*, **2002**,**124**:2568-2583

[12]Bu X H, Chen W, Du M, et al. *Inorg. Chem.*, **2002**,**41**:437-439

[13]Kasai K, Aoyagi M, Fujita M. *J. Am. Chem. Soc.*, **2000**,**122**: 2140-2141

[14]Sun L B, Li Y, Liang Z Q, et al. *Dalton Trans.*, **2012**,**41**: 12790-12796

[15]Li X M, Pan Y R, Ji J Y, et al. *J. Inorg. Organomet. Polym.*, **2014**,**24**:836-841

[16]Pan Y R, Sun M, Li X M. *Chin. J. Struct. Chem.*, **2015**,**34**: 576-584

[17]Liu Y Y, Ma J F, Yang Y, et al. *Inorg. Chem.*, **2007**,**46**: 3027-3037

[18]Sheldrick G M. *SHELXS*-97, *Program for the Solution of Crystal Structure*, University of Göttingen, Germany, **1997**.

[19]Sheldrick G M. *SHELXL*-97, *Program for the Refinement of Crystal Structure*, University of Göttingen, Germany, **1997**.

[20]Devereux M, Shea D O, Kellett A, et al. *Inorg. Biochem.*, **2007**,**101**:881-892

[21]Farrugia L J, Wing X A. *Windows Program for Crystal Structure Analysis*, University of Glasgow, UK, **1988**.

[22]Fu Z Y, Wu X T, Dai J C, et al. *Eur. J. Inorg. Chem.*, **2002**, **2002**:2730-2735

[23]Nakamoto K. *Infrared Spectra and Raman Spectra of Inorganic and Coordination Compound*. New York: Wiley, **1986.**

[24]Krische M J, Lehn J M. *Struct. Bond.*, **2000**,**96**:3-29

[25]Gilbert A, Baggott J. *Essentials of Molecular Photochemistry*. Oxford, Boston: Blackwell Scientific Publications, **1991**.

[26]Han Z B, He Y K, Ge C H, et al. *Dalton Trans.*, **2007**,**36**: 3020-3024

[27]Rendell D. *Fluorescence and Phosphorescence*. New York: John Willey & Sons, **1987**.

[28]Zheng S L, Chen X M. *Aust. J. Chem.*, **2004**,**57**:703-712

[29]Mohamed G G, El-Gamel N E A. *Spectrochim. Acta Part A*, **2004**,**60**:3141-3154

[30]Dong M N, He L L, Fan Y J, et al. *Cryst. Growth Des.*, **2013**,**13**:3353-3364

[31]Glasson C R K, Meehan G V, Motti C A, et al. *Dalton Trans.*, **2011**,**40**:10481-10490

[32]Pandey S, Das S S, Singh A K, et al. *Dalton Trans.*, **2011**, **40**:10758-10768

[33]Frisch M J, Trucks G W, Schlegel H B, et al. *Gaussian* 09, *Rev*. B.09, Gaussian Inc., Pittsburgh, **2009**.

[34]Parr R G, Yang W. *Density Functional Theory of Atoms and Molecules*. Oxford: Oxford University Press, **1989**.

[35]Ernzerhof M, Scuseria G E. *J. Chem. Phys.*, **1999**,**110**:5029-5036

[36]Adamo C, Barone V. *J. Chem. Phys.*, **1999**,**110**:6158-6170

[37]Perdew J P, Burke K, Ernzerhof M. *Phys. Rev. Lett.*, **1996**, **77**:3865-3868

[38]Perdew J P, Burke K, Ernzerhof M. *Phys. Rev. Lett.*, **1997**, **78**:1396-1397

[39]Dunning T H, Hay P J. *Modern Theoretical Chemistry*: *Vol.* 3. New York: Plenum, **1976**:1-28

[40]Wang L, Zhao J, Ni L, et al. *J. Inorg. Gen. Chem.*, **2012**, **638**:224-230

[41]LI Zhang-Peng(李章朋), XING Yong-Heng(邢永恒), ZHANG Yuan-Hong(张元红), et al. *Acta Phys.-Chim. Sin.*(物理化学学报), **2009**,**25**(4):741-746